Cerium and neodymium co-precipitation in molten chloride by wet argon sparging

J.F. Vigier, C. Renard, A. Laplace, J. Lacquement, F. Abraham

Cerium and neodymium co-precipitation in molten chloride by wet argon sparging

J.F. Vigier, C. Renard, A. Laplace, J. Lacquement, F. Abraham

PII: S0022-3115(12)00456-4
DOI: http://dx.doi.org/10.1016/j.jnucmat.2012.08.039
Reference: NUMA 46619

To appear in: *Journal of Nuclear Materials*

Received Date: 13 June 2012
Accepted Date: 24 August 2012

Please cite this article as: J.F. Vigier, C. Renard, A. Laplace, J. Lacquement, F. Abraham, Cerium and neodymium co-precipitation in molten chloride by wet argon sparging, *Journal of Nuclear Materials* (2012), doi: http://dx.doi.org/10.1016/j.jnucmat.2012.08.039

Cerium and neodymium co-precipitation in molten chloride by wet argon sparging

J.F. Vigier[a,b], C. Renard[b], A. Laplace[a], J. Lacquement[c] and F. Abraham[b]

[a]CEA, Nuclear Energy Division, RadioChemistry & Processes Department, SCPS/LEPS, F-30207 Bagnols sur Cèze, France

[b]Unité de Catalyse et de Chimie du Solide, UCCS UMR CNRS 8181, Univ. Lille Nord de France, ENSCL-USTL, B.P. 90108, 59652 Villeneuve d'Ascq Cedex, France

[c]CEA, Nuclear Energy Division, DTEC/DIR, F-30207 Bagnols sur Cèze, France

Keywords: molten chloride, co-precipitation, wet argon, oxychloride, solid solution.

Abstract

Co-precipitations of cerium (III) and neodymium (III) at 10 wt% in LiCl-$CaCl_2$ (30-70 mol%) molten salt at 705°C have been achieved using an original way of precipitation, wet argon sparging. Several $CeCl_3$/$NdCl_3$ ratios have been studied, and the isolated powders were analyzed using different characterization methods including XRD investigations. The lanthanides precipitation yield have been determined around 99.9 % using ICP analysis. XRD demonstrated that the precipitates mainly contained mixed oxychloride $(Ce_{1-x}Nd_x)OCl$ and a small amount of the mixed oxide $Ce_{1-y}Nd_yO_{2-0.5y}$. Calcination of these precipitates has resulted in the cerium and neodymium mixed oxides. For the precipitation with a Ce/Nd=50/50 ratio, an hydroxychloride $Ln(OH)_2Cl$ and the oxychloride $Ce^{IV}(Nd_{0.7}Ce_{0.3})^{III}O_3Cl$ have been identified as unexpected intermediate compounds.

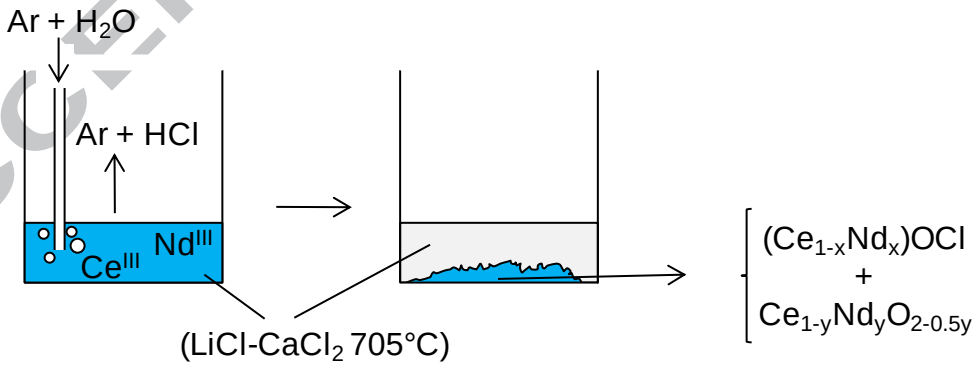

1. Introduction

Currently in France, spent nuclear fuel is recycled at industrial scale by the hydrometallurgical PUREX process which allows the selective recovery of uranium and plutonium. In the future, one of the different fuel cycle options under evaluation for Generation IV systems is co-management of the actinides (An) in an integrated closed fuel cycle [1]. Pyrochemical processes are sensed by the "*Commissariat à*

l'Energie Atomique" (CEA) as a potential alternative to hydrometallurgy [2]. The process being developed at the laboratory scale in CEA-ATALANTE facility is based on the oxide fuel dissolution in a molten fluoride media, followed by a grouped extraction of the actinides in a fused copper-aluminum phase [3]. Oxidative back-extraction allows to recover actinides as An(III) in the molten chloride LiCl-$CaCl_2$ (30-70 mol%) [4]. Then, the considered end-step of the process consists in the actinides co-precipitation, if possible in an oxide solid solution, in order to refabricate homogeneous new fuel. The present work consists of studying the precipitation in the molten LiCl-$CaCl_2$ (30-70 mol%) by using lanthanides (cerium and neodymium) as actinides surrogates.

Precipitation in molten chloride can be achieved by increasing the O^{2-} ion concentration in the salt. This is generally performed by adding oxo-donor solids like alkaline or alkaline-earth oxides or carbonates [5,6] or by oxobasic gases sparging [7]. The first method is not convenient because of the increasing quantity and the changing composition of the molten salt. The second method is generally achieved by sparging oxygen in the media [8]. However, oxygen is a too strong oxidant for uranium which precipitates in the form of oxides with higher oxidation states than the target UO_2 oxide or as uranates [9,10]. To our knowledge, there is no study on the precipitation process based on wet argon sparging which is less oxidative than oxygen and which does not change the cationic molten salt composition. Reaction of water in the molten chloride can be described as Equation 1.

$$H_2O_{(g)} + 2\ Cl^-_{(salt)} = O^{2-}_{(salt)} + 2\ HCl_{(g)} \quad (1)$$

The investigations on lanthanides precipitation in molten chloride are reported in the literature, generally in the frame of molten salt decontamination from fission products. The results reported on cerium and neodymium indicate a precipitation of these elements as oxychlorides, CeOCl by using Na_2CO_3 or BaO [5] and NdOCl with O_2 [9,10]. With oxygen sparging precipitation, cerium precipitates as CeO_2 [11, 7, 8]. Y.Z. Cho *et al.* [12,13] present the co-precipitation of several rare-earth elements by oxygen sparging. The oxychloride solid solution existence with many lanthanides was seen only by EDS, and no solid solution formation between cerium and neodymium was detected.

A detailed investigation was undertaken here on the co-precipitation of these two elements with wet argon sparging to determine the performance of the precipitation method and to examine solid solution formation. Therefore, precipitations were carried out with different x_{Nd} = Nd/(Ce+Nd) molar ratios including 0, 0.25, 0.50, 0.6, 0.75, 0.9 and 1. For each experiment, the precipitation yield was determined and the precipitate characterized (chemical composition and structure).

2. Experimental

2.1. Synthesis

The precipitations of Ln(III) (Ln=Ce and/or Nd) at 10 wt% in molten LiCl-$CaCl_2$ (30-70 mol%) heated to 705°C were done by wet argon sparging. The x_{Nd} = Nd/(Ce+Nd) molar ratios studied were 0, 0.25, 0.50, 0.60, 0.75, 0.90 and 1. The reactants, LiCl (Sigma Aldrich 99 %), $CaCl_2$ (Alpha Aesar 96 %), $NdCl_3.6H_2O$ (Sigma Aldrich 99.9 %), and $CeCl_3.7H_2O$ (Sigma Aldrich 99.9 %), were weighted to obtain 20 g of mixture after dehydration, with the different ratios of Ce and Nd. All the reactants were mixed and put in an alumina crucible. The experimental device used for precipitation is schematized in Figure 1. The crucible was placed in a leak tight quartz reactor, and finally this reactor placed in a furnace. The mixtures were first dehydrated by heating under vacuum at 150°C during 6 h. The temperature was maintained for 12 h at 150°C under dry argon atmosphere and then heated to 705°C (2°C/min), the complete fusion of the salt occurring at 680°C [14]. Wet argon was obtained by argon sparging in water, in a wash bottle with a PTFE frit, at 25°C upstream of the reactor at 2 $NL.h^{-1}$ flow rate. The saturation pressure of water vapor in this condition is 3169 Pa [15]. Then the precipitation was realized by sparging this gas in the molten chloride for 8 h. The reaction of water in the fused salt produced hydrochloric acid gas (Equation 1) neutralized downstream by a 1 M NaOH solution bubbler. After the end of precipitation, a top outlet of the reactor is open and a sample of molten salt was extracted from hot mixture by suction, using a quartz tube. Afterward, the reactor was cooled down to room temperature, the salt contained in the crucible was dissolved in water and the precipitate isolated by filtration. Each precipitate was calcined by heating in air at 1250°C for 24 h to convert it into oxides.

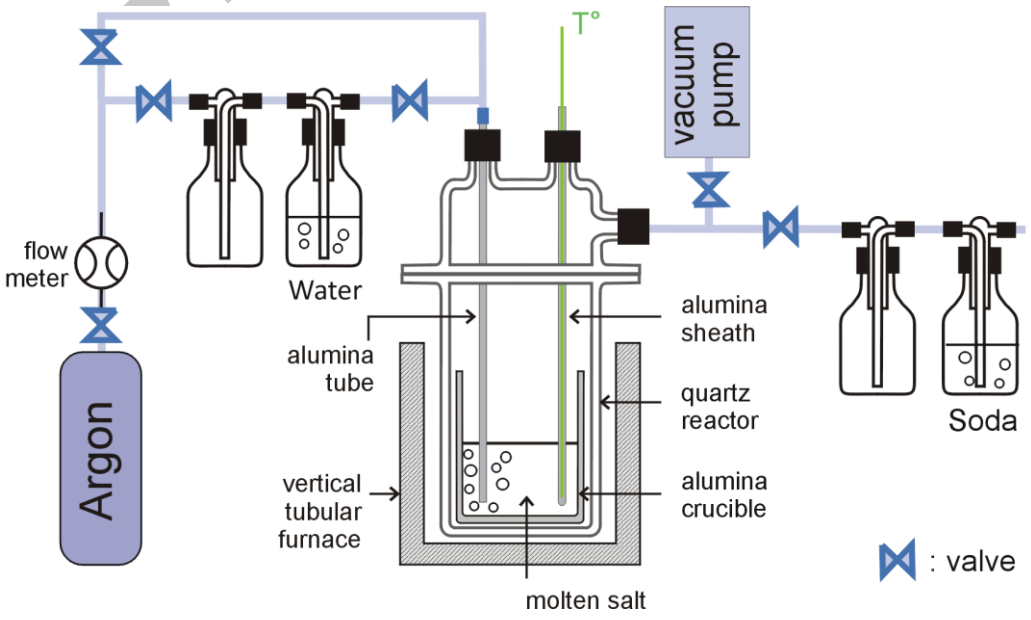

Figure 1 : Experimental device for cerium and neodymium precipitation in molten LiCl-$CaCl_2$ by humid argon sparging.

2.2. Analytical techniques

2.2.1. X-ray diffraction

The powder X-ray diffraction patterns of the precipitates were recorded with a Huber G670 Guinier powder diffractometer with transmission geometry using $Cu_{K\alpha 1}$ radiation isolated by a monochromator.

Powder diffraction patterns of calcined precipitates were recorded using a D8 Advance Bruker diffractometer with $Cu_{K\alpha}$ radiation and an energy dispersive detector (sol-X), over a 2θ range of 10°-80° at 0.02° increments. The profile fitting and the cell parameters refinements were performed using the powder option of JANA2006 [16].

2.2.2. Induced coupled plasma analysis (ICP-AES)

The precipitation rates were calculated from the concentration of soluble lanthanides remaining in the molten salt at the end of the precipitation. The concentrations of soluble cerium and neodymium in the salt were measured by Induced Coupled Plasma Atomic Emission Spectroscopy (ICP-AES). About 100 mg of samples extracted from the hot mixture at the end of the precipitation were dissolved in 100 mL of water and filtered to remove any precipitate. The acidification of the solution with nitric acid stabilized the solubilized elements. The analyses of the solutions gave the amount of unreacted lanthanides in the molten salt. To avoid matrix effect on the ICP-AES, the standard range was made with the same concentration of LiCl, $CaCl_2$ and HNO_3.

2.2.3. Electron probe microanalysis (EPMA)

To obtained an elemental map of the precipitate, the powder from the $x_{Nd} = 0.5$ ratio was placed in a resin and polished, and then analyzed in a Castaing microprobe (CAMECA SX100) by wavelength dispersive spectrometry (WDS).

2.2.4. Scanning electron microscope (SEM)

The morphology of the precipitate was observed with a Scanning Electron Microscope (SEM) Hitachi S4700 with Field Emission Gun (FEG), a cathodoluminescence and an Electron Beam Induced Current (EBIC) system.

2.2.5. Conductimetric analysis.

The neutralization of the hydrogen chloride from water reaction leads to a decrease of the soda conductivity. The water reaction in the molten salt was followed up with the measurement of the conductivity of the soda solution placed downstream the reactor.

$$HCl_{(g)} + OH^- + Na^+ \rightarrow H_2O + Na^+ + Cl^- \quad (2)$$

With a known flow rate and water temperature upstream of the reactor, the maximal hydrochloric acid flow rate and the theoretical conductivity evolution were calculated. The water molar flow rate, D_{H_2O} , was calculated with the ideal gas relation :

$$P^{sat}_{H_2O} D = D_{H_2O} RT \quad (3)$$

with $P^{sat}_{H_2O}$ the partial vapor pressure of water and D is the wet argon flow rate. According to equation (1), the maximal molar flow rate of HCl is:

$$D_{HCl} = 2D_{H_2O} \quad (4)$$

The theoretical conductivity evolution was calculated according to Kohlrausch's law, using the cations and anions molar conductivity and equation (2). The calculated values are given in Table 1.

experimental data		calculated data	
Ar flow rate, D	2 $L.h^{-1}$	H_2O partial vapor pressure, $P^{sat}_{H_2O}$	3169 Pa
H_2O temperature	25°C	H_2O molar flow rate, D_{H_2O}	0.00256 $mol.h^{-1}$
NaOH solution volume	500 mL	Maximal HCl molar flow rate	0.00512 $mol.h^{-1}$
NaOH solution concentraion	1 M	Highest conductivity evolution	-1.25 $mS.cm^{-1}.h^{-1}$

Table 1: Experimental and calculated data for precipitation and the maximal conductivity evolution of the soda solution downstream the reactor.

3. Results and discussion

3.1. Precipitation yield

The evolution of soda solution conductivity shown in Figure 2 is close to that calculated using the parameters given in Table 1, indicating that all the water introduced by the wet argon is reacting in the molten salt. This demonstrates the high reactivity of water in these conditions. In addition, this evolution confirms the water vapor saturation of argon.

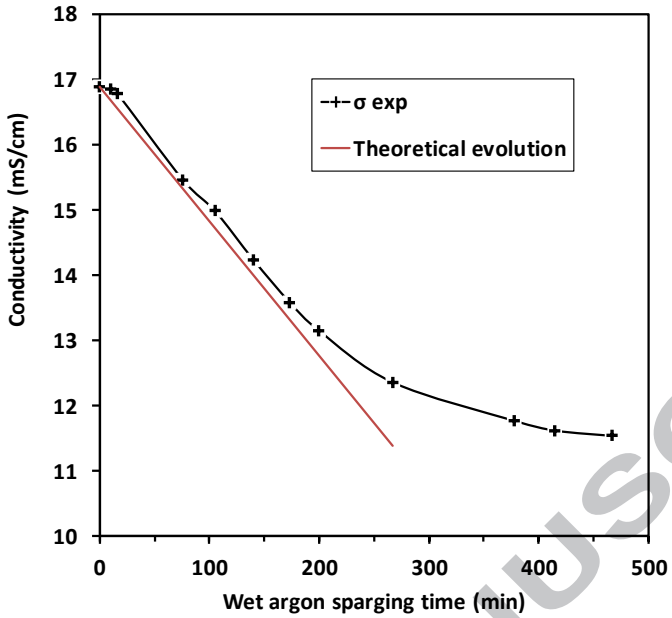

Figure 2: Evolution of soda solution conductivity downstream the precipitation reactor for the ratio x_{Nd} = 0.5. t=0 corresponds to the beginning of wet argon sparging.

ICP-AES analysis of unreacted lanthanides in the LiCl-$CaCl_2$ salt after the end of precipitation showed only neodymium and cerium traces, near the apparatus detection limit (< 0.1 ppm, corresponding to a yield >99.9%). The reaction is quantitative with a precipitation yield about 99.9 % (Table 2).

X_{Nd}	Ce precipitation yield (%)	Nd precipitation yield (%)
0.00	99.90(5)	-
0.25	99.80(5)	99.90(5)
0.50	99.90(5)	99.90(5)
0.75	99.90(5)	100.00(5)
1.00	-	99.90(5)

Table 2: Cerium and neodymium precipitation yields after 8 h wet argon sparging, determined by ICP-AES analysis of unreacted cerium and neodymium.

3.2. Precipitates characterization

The XRD patterns of the precipitates reveal the formation of a mixture of CeOCl oxychloride and CeO_2 oxide, and NdOCl oxychloride for x_{Nd} = 0 and 1, respectively (Figure 3). Cerium oxide formation is due to oxidation of some of the cerium from oxidation state (III) to (IV). The precipitation using wet argon is partially oxidative, which can be explained by the presence of hydroxide ions in molten salt [17]:

$$OH^-_{(salt)} + e^- = O^{2-} + ½\ H_2 \qquad (5)$$

CeOCl and NdOCl crystallize with the same PbClF type structure [18]. In the case of cerium/neodymium co-precipitation, the low 2θ shift of the oxychloride diffraction peaks with the increase of cerium concentration clearly indicates the formation of a solid solution $(Ce_{1-x}Nd_x)OCl$ [19]. This shift is caused by the greater ionic radius of Ce(III) than Nd(III) [20]. Conversely, the high 2θ shift of the oxide diffraction peaks with the increase of cerium concentration is caused by a smaller ionic radius of Ce(IV) than Nd(III), and demonstrates the formation of $Ce_{1-y}Nd_yO_{2-0.5y}$ solid solutions. The cell parameter refinement of the fluorite-type oxide phase (Table 3) allows the determination of the neodymium/cerium proportion. Besides, it shows a high cerium concentration in the oxide phase compared to the initial Ce/Nd proportion in the molten chloride. However, even if the neodymium concentration is limited in the oxide, this result is remarkable because of the oxobasic nature of neodymium oxide in molten chloride [21] (Equation 4). This property has been verified in this study by introduction of neodymium oxide in molten LiCl-$CaCl_2$ (30-70 mol%) at 705°C. The powder isolated after cooling the salt to room temperature was identified as NdOCl by XRD analysis. Neodymium oxide was not detected and is therefore not stable in LiCl-$CaCl_2$.

$$Nd_2O_3 + Cl^-_{(salt)} \rightarrow NdOCl + O^{2-}_{(salt)} \quad (6)$$

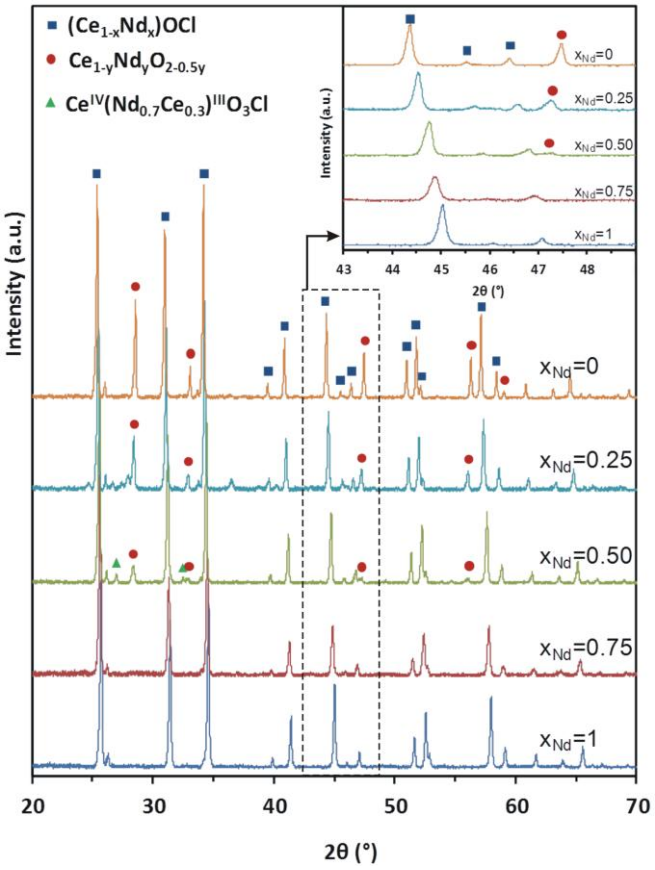

Figure 3: XRD patterns obtained for the precipitates and coprecipitates of cerium and neodymium from molten LiCl-$CaCl_2$ (30-70 mol%). x_{Nd} is the initial lanthanide composition in the molten salt.

X_{Nd}	refined Cell parameter of oxides $Ce_{1-y}Nd_yO_{2-0.5y}$	y value of $Ce_{1-y}Nd_yO_{2-0.5y}$ deduced from [22,23]
0.00	5.4106(4)	0
0.25	5.4364(2)	0.15-0.12
0.50	5.4457(6)	0.20-0.17
0.60	5.4595(6)	0.29-0.25

Table 3: Refinement cell parameters of oxides $Ce_{1-y}Nd_yO_{2-0.5y}$ from precipitation and deduced y values.

The SEM pictures of the precipitate for x_{Nd} = 0.5 (Figure 4) reveal two crystal morphologies: irregular plate crystals with few tens of micrometers sides corresponding to the oxychloride and reminding its tetragonal structure, and parallelepipedic crystals with few micrometers sides corresponding to the oxide and reminding its fluorite structure.

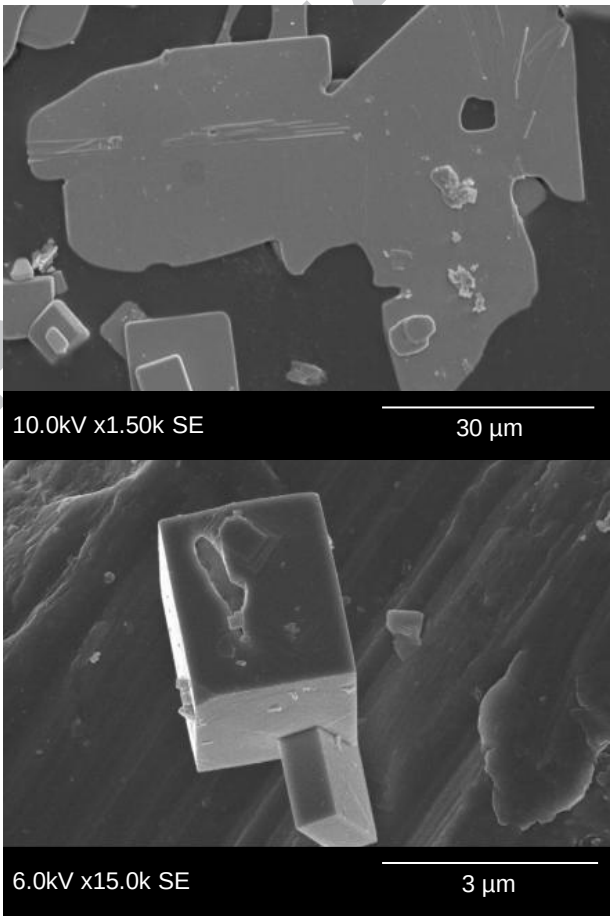

Figure 4: SEM pictures of the x_{Nd} = 0.5 precipitate showing the $(Ce_{1-x}Nd_x)OCl$ (top) and $Ce_{1-y}Nd_yO_{2-0.5y}$ (bottom) morphologies.

The microprobe cartography (Figure 5) of the precipitate from the x_{Nd} = 0.5 shows the presence of cerium, neodymium and chloride in the same crystals confirming the formation of mixed oxychloride $(Ce_{1-x}Nd_x)OCl$, and high concentration of cerium, low concentration of neodymium and no presence of chlorine in some crystals confirming the formation of rich cerium mixed oxide $Ce_{1-y}Nd_yO_{2-0.5y}$.

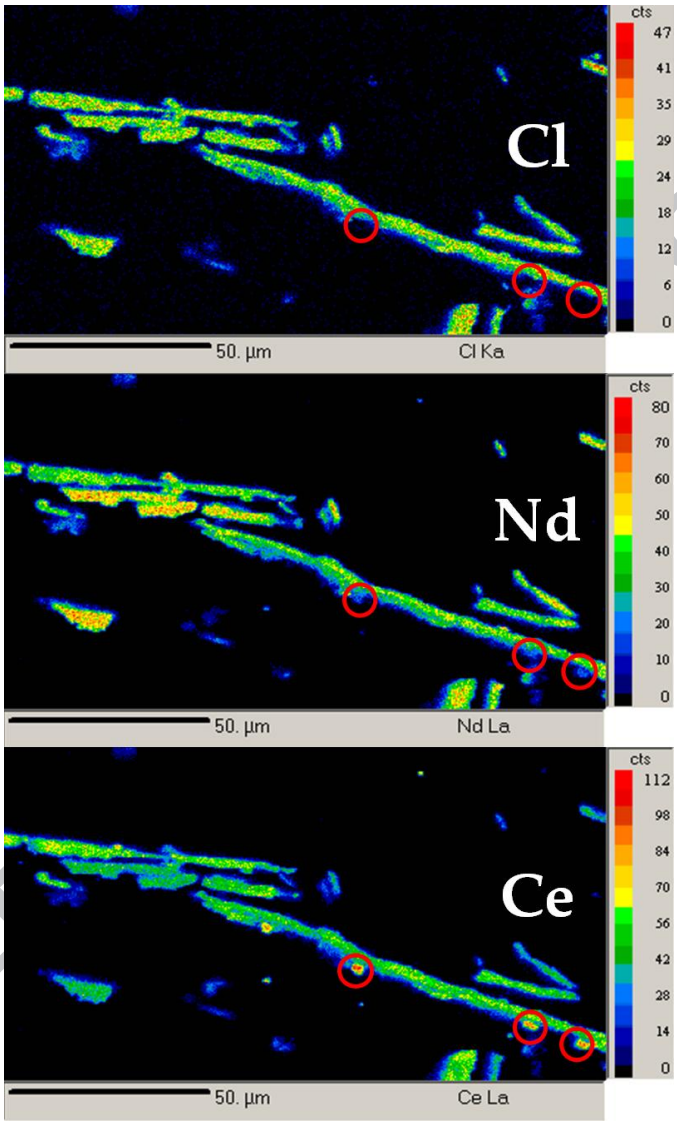

Figure 5: Chlorine (Cl), neodymium (Nd) en cerium (Ce) cartography from microprobe analysis of x_{Nd}=0.5 precipitate. Red circles point out $Ce_{1-y}Nd_yO_{2-0.5y}$ mixed oxide.

The oxychloride $(Ce_{1-x}Nd_x)OCl$ has a good solubility in dilute acid while mixed oxide $Ce_{1-y}Nd_yO_{2-0.5y}$ is not soluble in this condition. The proportion of oxide in each precipitate was evaluated by selective dissolution of oxychloride, in HCl 0.1M, and by weighing of the un-dissolved powder. Figure 6 shows the oxide/oxychloride distribution in weight, in the precipitate, as a function of the initial Nd/(Nd+Ce) molar ratio in the molten salt. The oxide content is around 20 % for the precipitation of pure cerium and decreases with the increase of neodymium proportion to less than 1 % for $x_{Nd} \geq 0.75$.

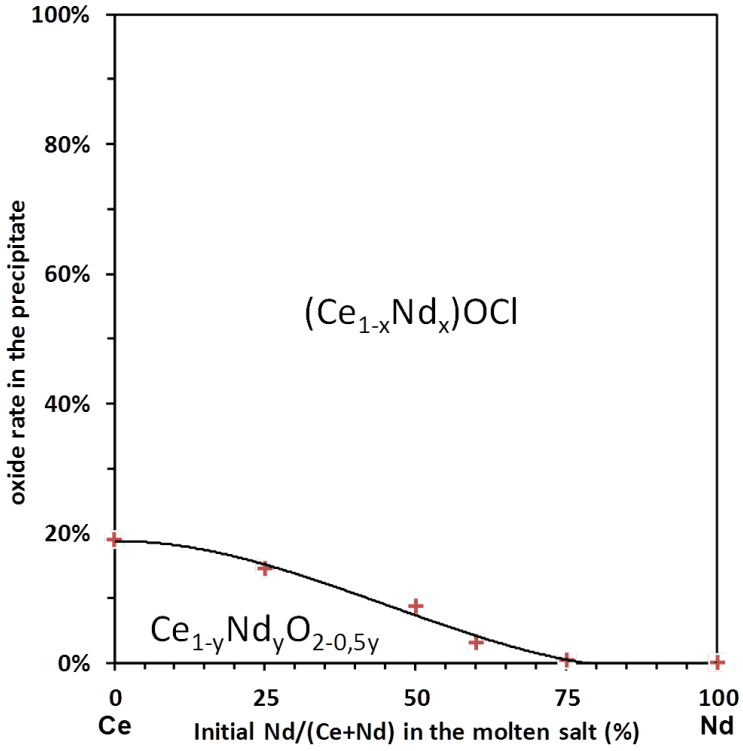

Figure 6: Oxychloride $(Ce_{1-x}Nd_x)OCl$ and oxide $Ce_{1-y}Nd_yO_{2-0.5y}$ distribution depending on the initial lanthanide composition of the salt.

Because of possible calcium contamination in the precipitate which could be problematic in the fuel refabrication, the concentration of this element has been determined by ICP-AES analysis of solubilized precipitates. The calcium represents 0.1 wt% in the different analyzed precipitates, except for the pure neodymium precipitate where no calcium was detected. Therefore, calcium contamination is probably mainly located in the oxide, which can integrate Ca in the cerine structure $Ce_{1-x}Ca_xO_{2-x}$ [24].

3.3. Precipitates calcination

The calcination of the mixed oxychloride $(Ce_{1-x}Nd_x)OCl$ at 1250°C for 24 h under air atmosphere produces reactions (7), (8) or (9) and gives, ,according to the XRD analysis, the Nd_2O_3 and CeO_2, and the fluorite-type solid solution $Ce_{1-x}Nd_xO_{2-0.5x}$, respectively.

$$2\ NdOCl + ½\ O_{2(g)} \rightarrow Nd_2O_3 + Cl_{2(g)} \quad (7)$$

$$CeOCl + ½\ O_{2(g)} \rightarrow CeO_2 + ½\ Cl_{2(g)} \quad (8)$$

$$Ce_{1-x}Nd_xOCl + 0.25(2-x)\ O_{2(g)} \rightarrow Ce_{1-x}Nd_xO_{2-0.5x} + ½\ Cl_{2(g)} \quad (9)$$

For x_{Nd} = 0.25 to 0.5, the X-ray diffraction patterns show two distinct cerium neodymium mixed oxides: $Ce_{1-x}Nd_xO_{2-0.5x}$, produced by the oxychloride calcination, and $Ce_{1-y}Nd_yO_{2-0.5y}$, obtained during the precipitation. There is no diffusion at 1250°C

between the mixed oxide $Ce_{1-y}Nd_yO_{2-0.5y}$ coming from precipitation and the mixed oxide $Ce_{1-x}Nd_xO_{2-0.5x}$ coming from oxychloride conversion.

The cerium/neodymium mixed oxides have been previously investigated by several authors [22,23,24,25]. With the increase of neodymium concentration, the mixed oxide structure changes from fluorine F-type ($Fm\bar{3}m$, with a_F unit cell parameter) to the superstructure C-type ($Ia\bar{3}$, $a_C \approx 2a_F$ unit cell parameter) at about $x_{Nd}\approx0.40$. Above $x_{Nd}\approx0.75$, $Ce_{0.25}Nd_{0.75}O_{1.625}$ C-type and Nd_2O_3 A-type coexist. The results obtained from the XRD analysis of the calcined precipitates (Figure 7) are in agreement with these different studies and confirm the conversion of mixed oxychlorides into mixed oxides under calcination.

The evolution of the cell parameter refined from the X-ray diffraction patterns is in good agreement with data given in the literature [22,23,25] (Table 4, Figure 8) and with the results from the precipitate. The $Ce_{1-x}Nd_xO_{2-0.5x}$ mixed oxides coming from the oxychloride calcination contain, as the corresponding oxychloride, a neodymium ratio higher than the initial composition x_{Nd}. The samples with x_{Nd} = 0.75 and 0.90 reveal that, during calcinations the mixed oxychloride converts into two phases ; Nd_2O_3 and $Ce_{1-x}Nd_xO_{2-0.5x}$ C-type mixed oxide with x < 0.75 as confirmed by the refined unit cell parameter : a/2 = 5.5116(4) and 5.5242(4) Å respectively.

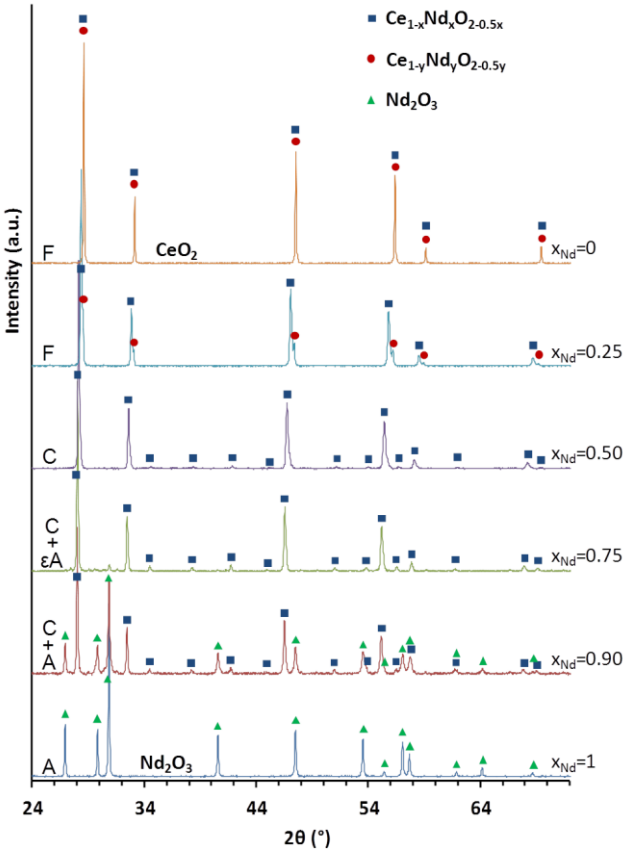

Figure 7: XRD patterns of calcined precipitates. $Ce_{1-y}Nd_yO_{2-0.5y}$ is the mixed oxide formed during precipitation, $Ce_{1-x}Nd_xO_{2-0.5x}$ and Nd_2O_3 are the mixed oxide and oxide from calcined oxychloride. F=F-type Fm $\bar{3}$ m structure, C=C-type Ia $\bar{3}$ structure, and A=A-type P $\bar{3}$ 1m structure. x_{Nd}=Nd/(Ce+Nd) molar ratio initially introduced in the molten salt.

Initial x_{Nd}	structure	Lattice parameter (Å)
0 .00	F-type *Fm* $\bar{3}$ *m*	a=5.4118(1)
0.25	F-type *Fm* $\bar{3}$ *m*	a=5.4654(1)
0.50	C-type *Ia* $\bar{3}$	a/2=5.4915(3)
0.75	C-type *Ia* $\bar{3}$	a/2=5.5116(4)
0.90	C-type *Ia* $\bar{3}$	a/2=5.5242(4)

Table 4: Refined unit cell parameter of $Ce_{1-x}Nd_xO_{2-0.5x}$ depending on the initial lanthanides composition of the salt.

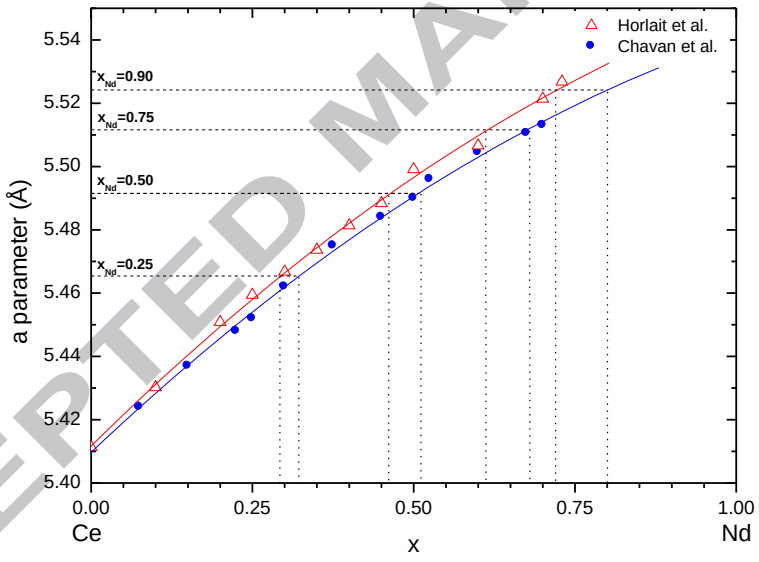

Figure 8: $Ce_{1-x}Nd_xO_{2-0.5x}$ unit cell parameter versus x substitution rate according to bibliography. The refined cell parameter of mixed oxide obtained from calcined precipitates are reported, x_{Nd} is the initial lanthanides composition of the salt.

3.4. Intermediate compounds during precipitation

The co-precipitation of a x_{Nd} = 0.5 experiment has been studied as a function of the precipitation time by extracting samples at various reaction duration. The experimental conditions were the same than those described in paragraph 2.1 but the duration of wet argon bubbling was 48 h. For each extraction, a top outlet of the reactor was open, a quartz tube was immersed in the molten salt and about 1 g of salt was aspired in the tube. Afterward, the precipitates contained in the samples

were isolated and analyzed by XRD (Figure 9). As previously observed, the final precipitate contains mixed oxychloride and mixed oxide. The precipitation occurs through two others species. Hydroxychloride $Ln(OH)_2Cl$ is formed with oxychloride at the beginning of the precipitation and is then quickly consumed. The oxychloride $Ce^{IV}(Nd_{0.7}Ce_{0.3})^{III}O_3Cl$ [26] appears at the beginning of the precipitation and is consumed after the end of precipitation. We can notice that the XRD patterns of the precipitate extracted after 8h35 is different from that of x_{Nd}=0.5 shown in Figure 3, the proportion of $Ce^{IV}(Nd_{0.7}Ce_{0.3})^{III}O_3Cl$ is higher in the first case. The formation of $Ce^{IV}(Nd_{0.7}Ce_{0.3})^{III}O_3Cl$ is probably enhanced by the opening of the outlet of the reactor at each sample extraction, inducing oxygen contamination, which can explain its unusual presence after 8h35. The mixed oxide $Ce_{1-y}Nd_yO_{2-0.5y}$ from precipitation appears at the end of precipitation, when the overall lanthanide concentration in the molten salt is below 1 wt% from ICP-AES analysis.

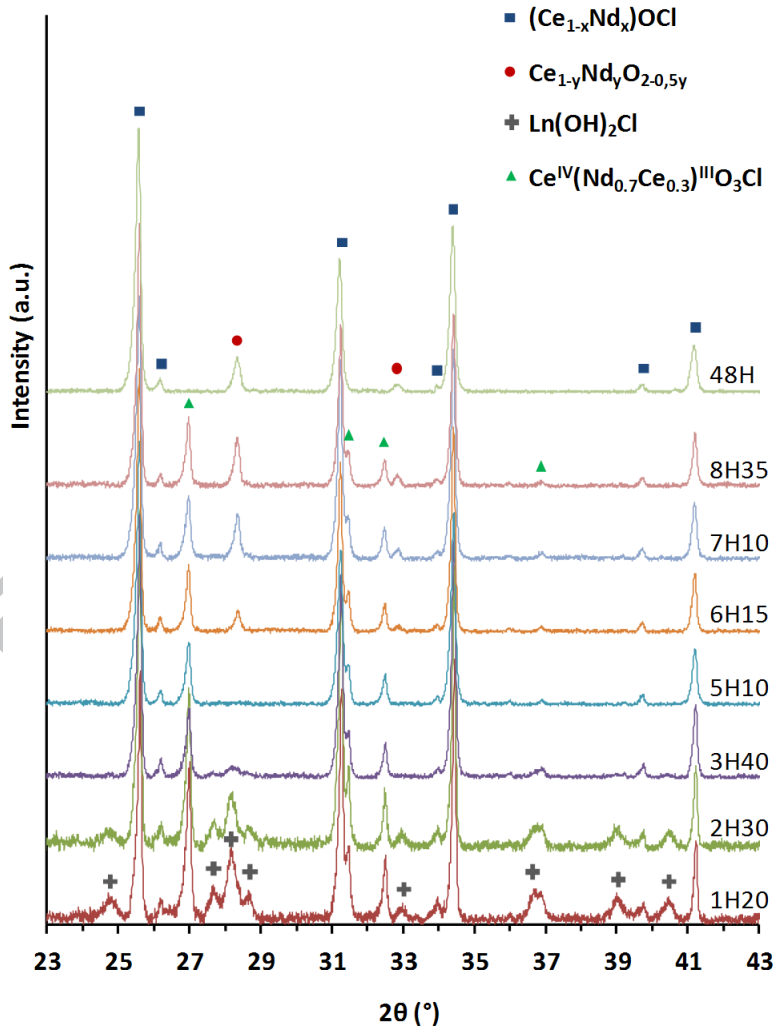

Figure 9: XRD patterns obtained for Ce/Nd coprecipitates with x_{Nd} = 0.5 in molten LiCl-$CaCl_2$ (30-70 mol%), depending on wet argon sparging time.

4. Conclusion

The precipitations of cerium and neodymium at 10 wt% in molten LiCl-$CaCl_2$ (30-70 mol%) at 705°C by wet argon sparging were investigated in order to characterize this precipitation route, and to demonstrate solid solution formation. In these conditions, water vapor is highly reactive, with a total reaction in the molten salt and a quantitative precipitation of the lanthanides with efficiency around 99.9 %. This precipitation method is partially oxidative with a small amount of Ce(III) oxidized to Ce(IV).

The co-precipitation of the two lanthanides mainly leads to mixed oxychloride $(Ce_{1-x}Nd_x)OCl$ formation which is converted to the respective mixed oxide $Ce_{1-x}Nd_xO_{2-0.5x}$ by calcination under air at 1250°C. Despite the oxobasicity of neodymium oxide in molten chlorides, the formation of mixed oxide $Ce_{1-y}Nd_yO_{2-0.5y}$ is detected in the precipitate with $x_{Nd}<0.75$. However, the neodymium concentration is smaller in this oxide and higher in the oxychloride than its initial content in the salt Two intermediate compounds have been detected during the precipitation for x_{Nd} = 0.5; an hydroxychloride $Ln(OH)_2Cl$ and the intergrowth oxychloride $Ce^{IV}(Nd_{0.7}Ce_{0.3})^{III}O_3Cl$. The former is more quickly consumed than the latter in the molten salt.

In the frame of the developed pyrochemical process, this technique of precipitation by wet argon sparging seems promising. It could be used for nuclear fuel refabrication in the process end-step. This method will be further tested with actinides in order to confirm the precipitation yield and to characterize the obtained powder.

Acknowledgment

This work was supported by the PARIS French Research Group included in the PACEN Program. The authors would like to thank Mrs. Nora Djelal and Laurence Burylo (UCCS, University of Lille) for their technical assistances.

References

[1] US DOE Nuclear Research and Advisory Committee and the Generation IV International Forum, A Technology Roadmap for Generation IV Nuclear Energy Systems, December 2002.

[2] J. Lacquement, H. Boussier, A. Laplace, O. Conocar, A. Grandjean, *J. Fluorine Chem.*, 130 (2009) 18-21.

[3] O. Conocar, N. Douyere, J. Lacquement, *J. Nucl. Mater.*, 344 (2005) 136-141.

[4] E. Mendes, O. Conocar, A. Laplace, N. Douyère, J. Lacquement, M. Miguirditchian, Procceding of molten salts chemistry and technology, MS-9, Trondheim, 2011.

[5] Y. Castrillejo, M.R. Bermejo, R. Pardo, A.M. Martinez, *J. Electroanal. Chem*., 522 (2002) 124-140.

[6] Y. Katayama, R. Hagiwara, Y. Ito, *J. Electrochem. Soc.*, 142 (1995) 2174-2178.

[7] H.C. Eun, Y.Z. Cho, H.S. Park, T.K. Lee, I.T. Kim, K.I. Park, H.S. Lee, *J. Nucl. Mater.*, 408 (2011) 110-115.

[8] H.C. Eun, Y.J. Cho, H.C. Yang, H.S. Park, E.H. Kim, I.T. Kim, *J. Radioanal. Nucl. Chem.*, 274 (2007) 621-624.

[9] L. Martinot, J. Fuger, *J. Less-Common Met.*, 120 (1986) 255-266.

[10] L. Martinot, M. Ligot, *J. Radioanal. Nucl. Chem. Lett.*, 136 (1989) 53-60.

[11] Y.J. Cho, H.C. Yang, H.C. Eun, E.H. Kim, I.T. Kim, *J. Nucl. Sci. Technol.*, 43 (2006) 1280-1286.

[12] Y.Z. Cho, G.H. Park, H.C. Yang, D.S. Han, H.S. Lee, I.T. Kim, *J. Nucl. Sci. Technol.*, 46 (2009) 1004-1011.

[13] Y.Z. Cho, H.C. Yang, G.H. Park, H.S. Lee, I.T. Kim, *J. Nucl. Mater.*, 384 (2009) 256-261.

[14] K.H. Mahendran, S. Nagaraj, R. Sridharan, T. Gnanasekaran, *J. Alloys Compd.*, 325 (2001) 78-83.

[15] D.R. Lide, Handbook of chemistry and physics 73rd Edition, 1992-1993.

[16] V. Petříček, M. Dušek, L. Palatinus, JANA2006, in, 2000, pp. The Crystallographic Computing System, Institute of Physics Academy of Sciences of the Czech Republic Praha.

[17] H.A. Laitinen, W.S. Ferguson, R.A. Osteryoung, *J. Electrochem. Soc.*, 104 (1957) 516-520.

[18] J. Hölsä, M. Lahtinen, M. Lastusaari, J. Valkonen, J. Viljanen, *J. Solid State Chem.*, 165 (2002) 48-55.

[19] J. Hölsä, E. Kestilä, K. Koski, H. Rahiala, *J. Alloys Compd.*, 225 (1995) 193-197.

[20] R. Shannon, *Acta Crystallogr. Sect. A: Found. Crystallogr.*, 32 (1976) 751-767.

[21] H. Hayashi, K. Minato, *J. Phys. Chem. Solids*, 66 (2005) 422-426.

[22] S.V. Chavan, M.D. Mathews, A.K. Tyagi, *Mater. Res. Bull.*, 40 (2005) 1558-1568.

[23] D. Horlait, L. Claparede, N. Clavier, S. Szenknect, N. Dacheux, J. Ravaux, R. Podor, *Inorg. Chem.*, 50 (2011) 7150-7161.

[24] B.C. Mohanty, J.W. Lee, D.H. Yeon, Y.H. Jo, J.H. Kim, Y.S. Cho, *Mater. Res. Bull.*, 46 (2011) 875-883.

[25] Y. Ikuma, E. Shimada, N. Okamura, *J. Am. Ceram. Soc.*, 88 (2005) 419-423.

[26] J.F. Vigier, C. Renard, N. Henry, A. Laplace, F. Abraham, *Inorg. Chem.,* 51(7) (2012) 4352–4358.

Figure 1

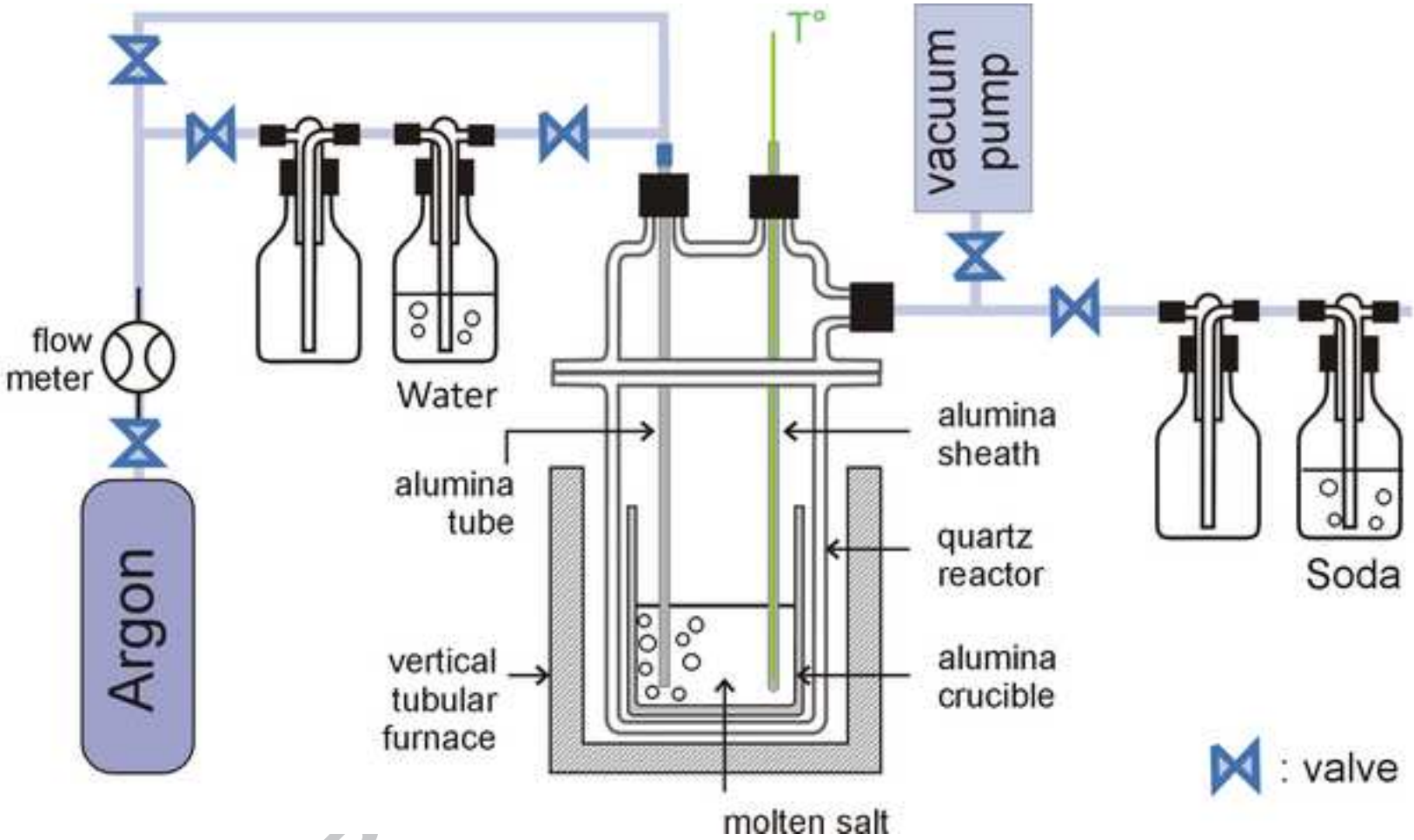

Figure 2

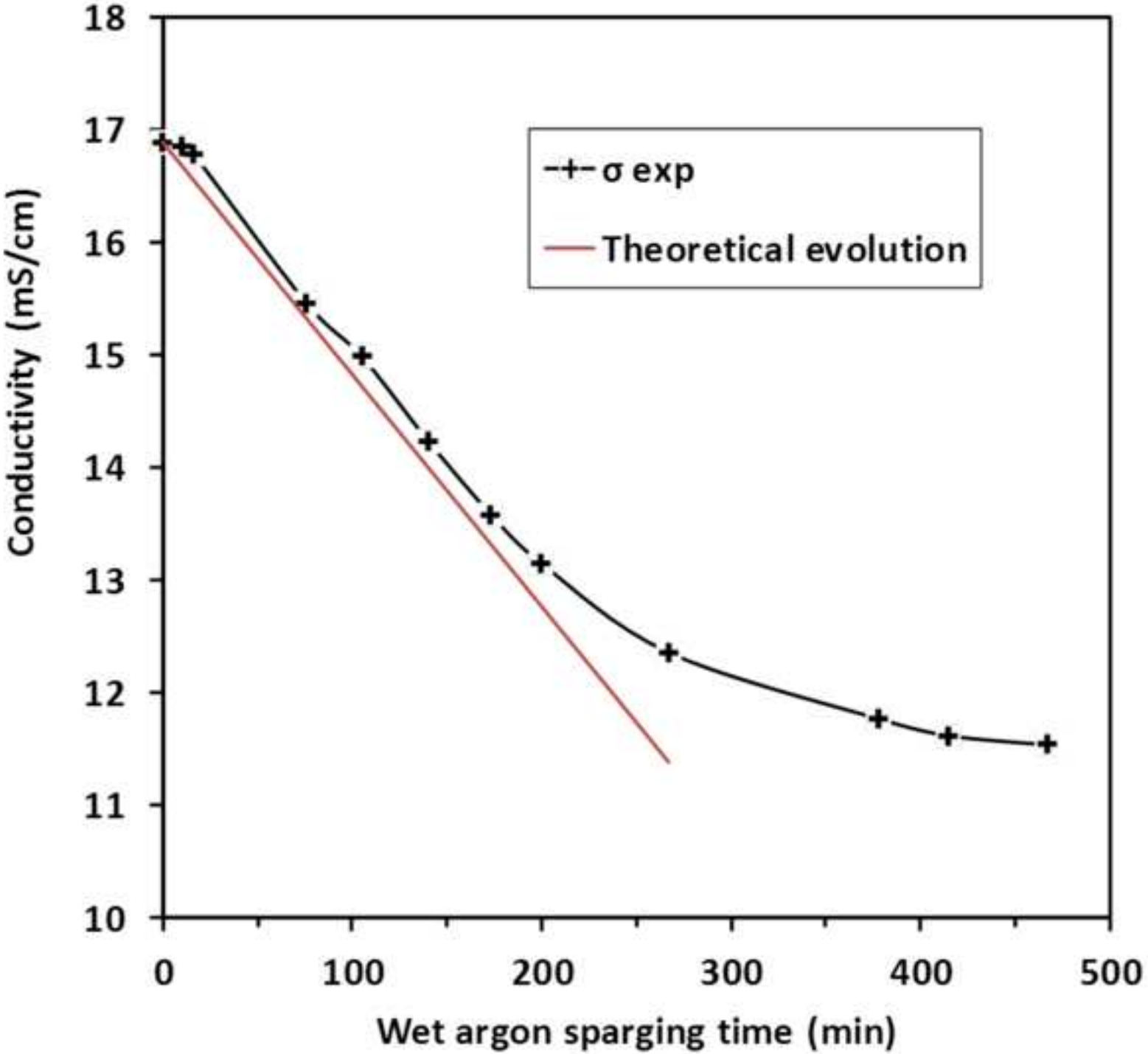

Figure 3

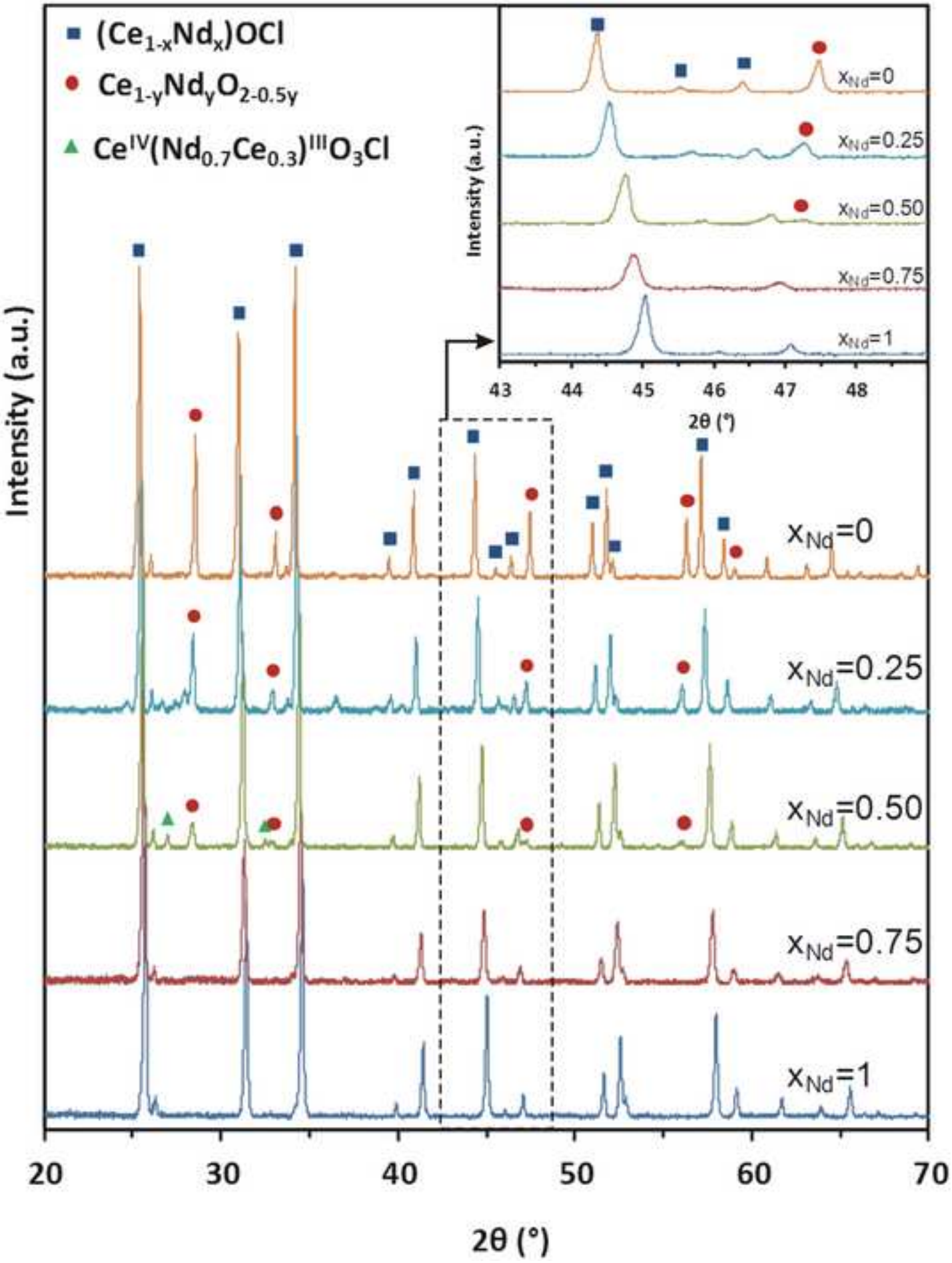

Figure 4

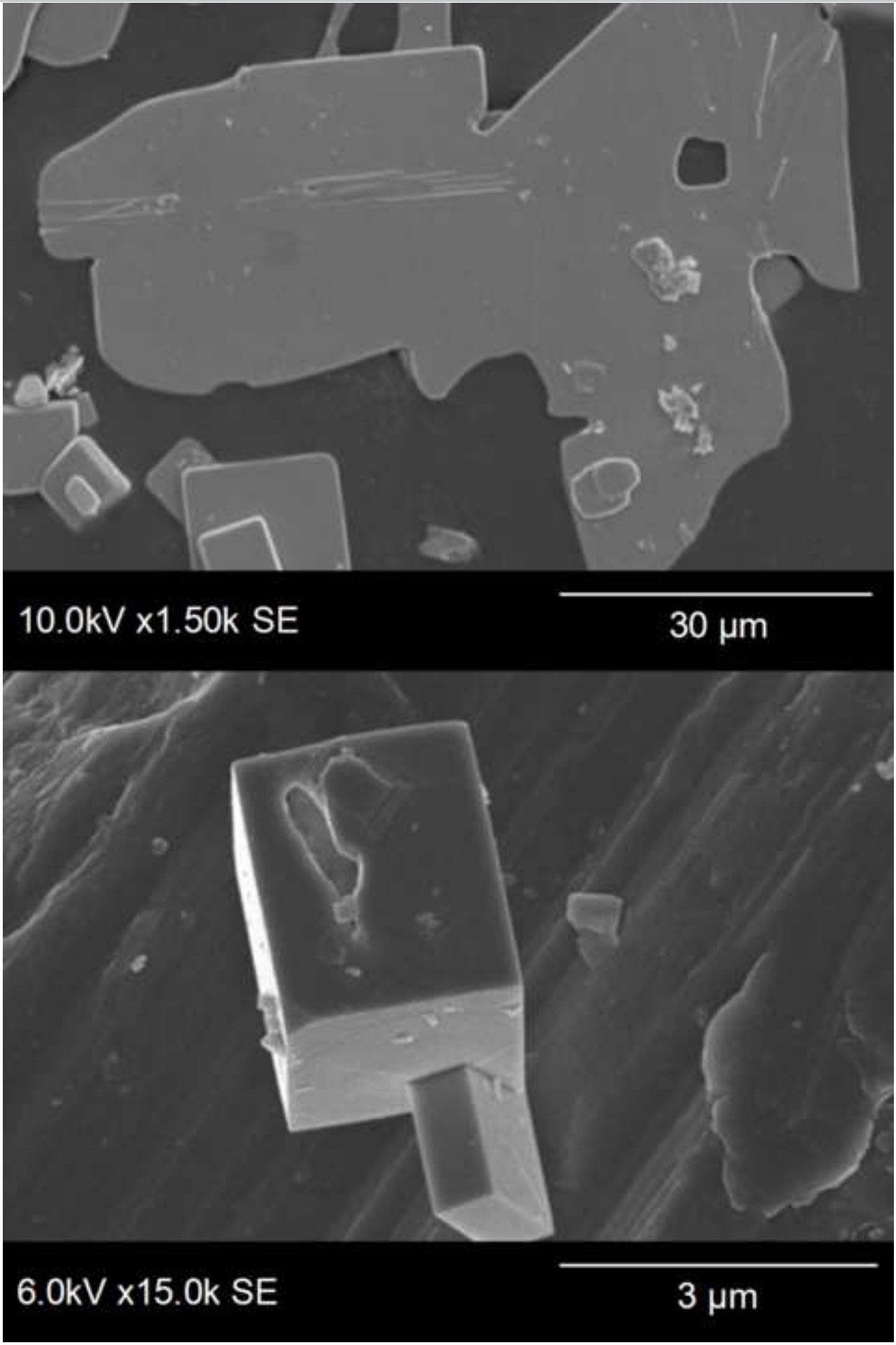

Figure 5

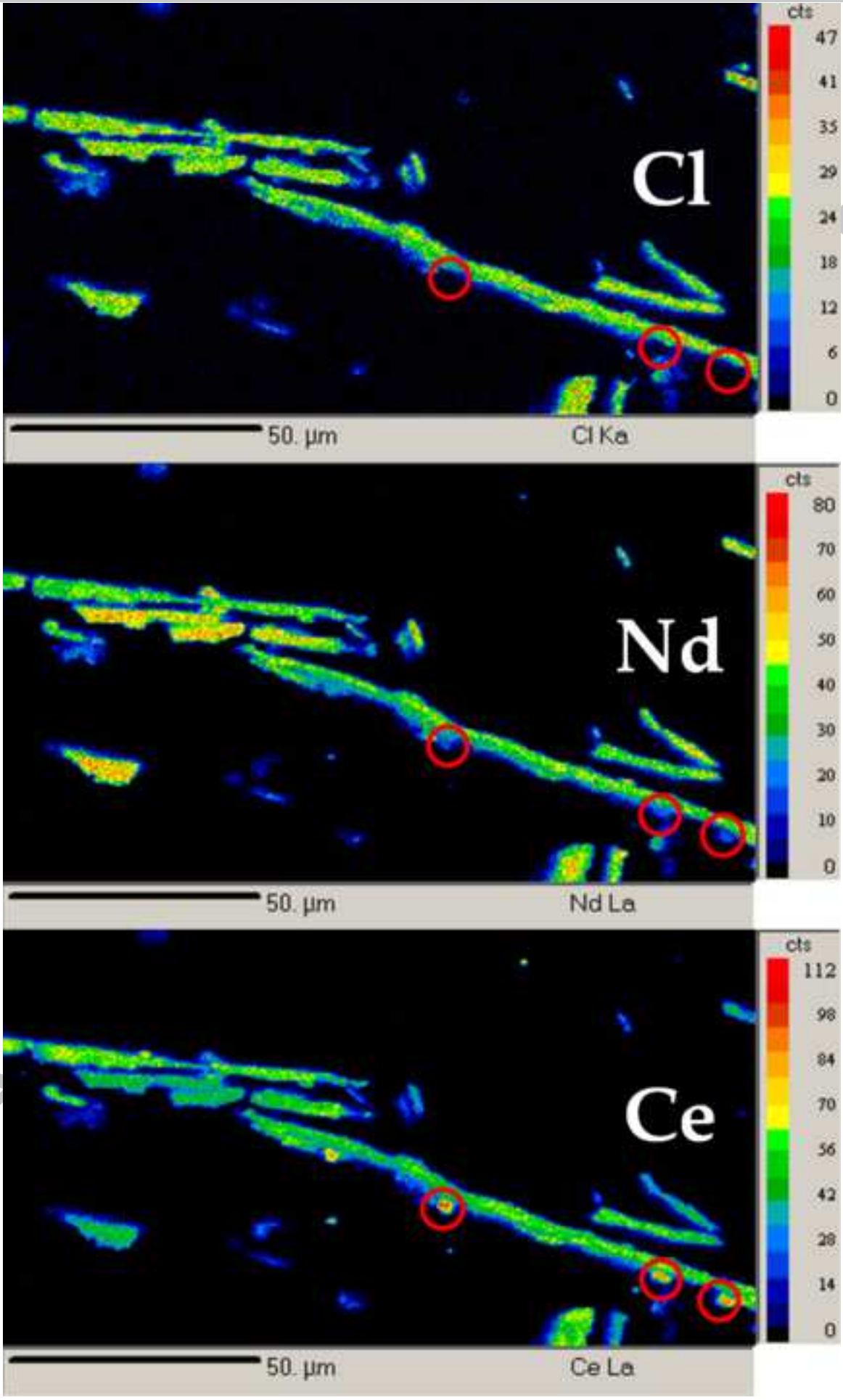

Figure 6

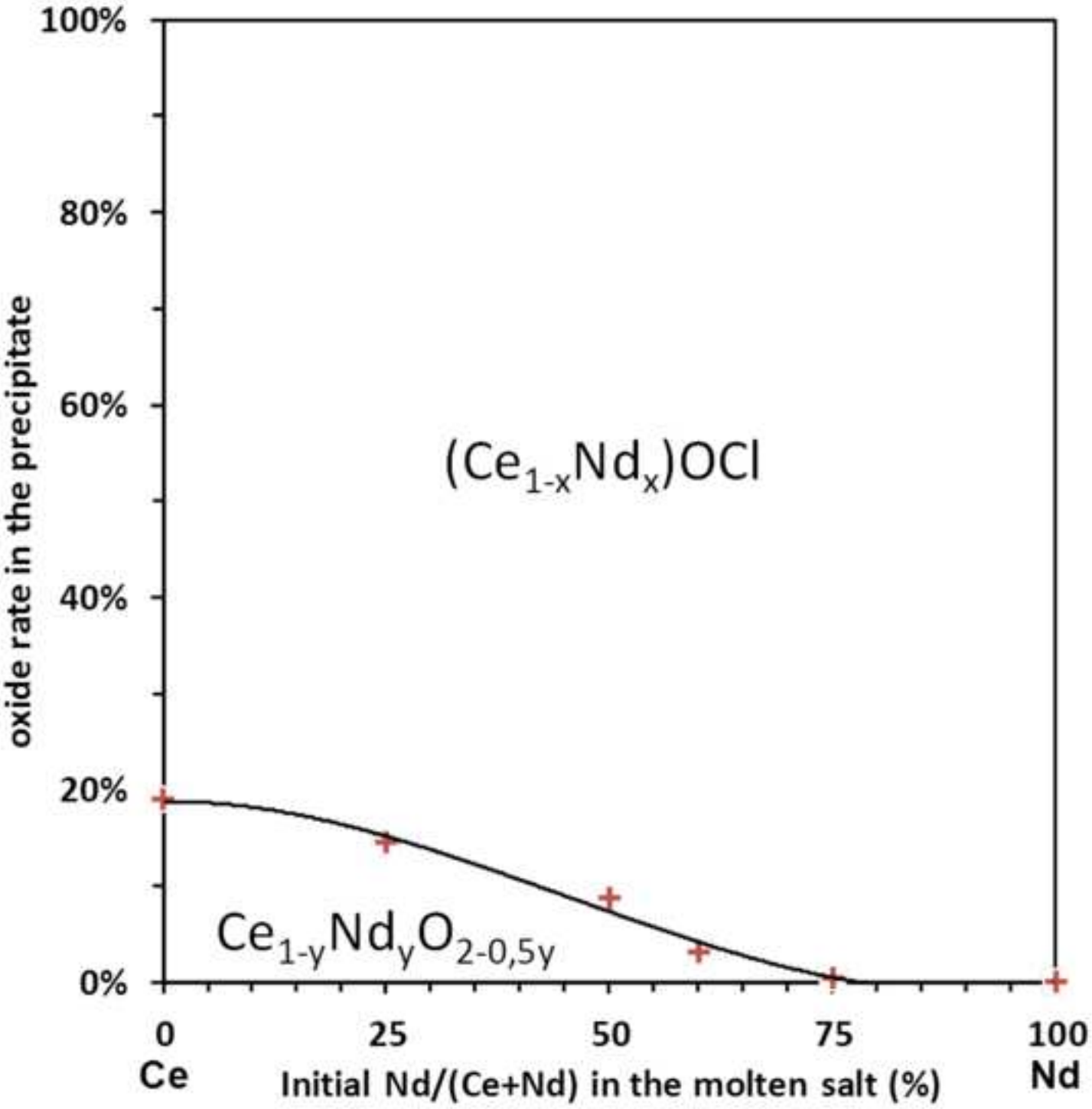

Figure 7

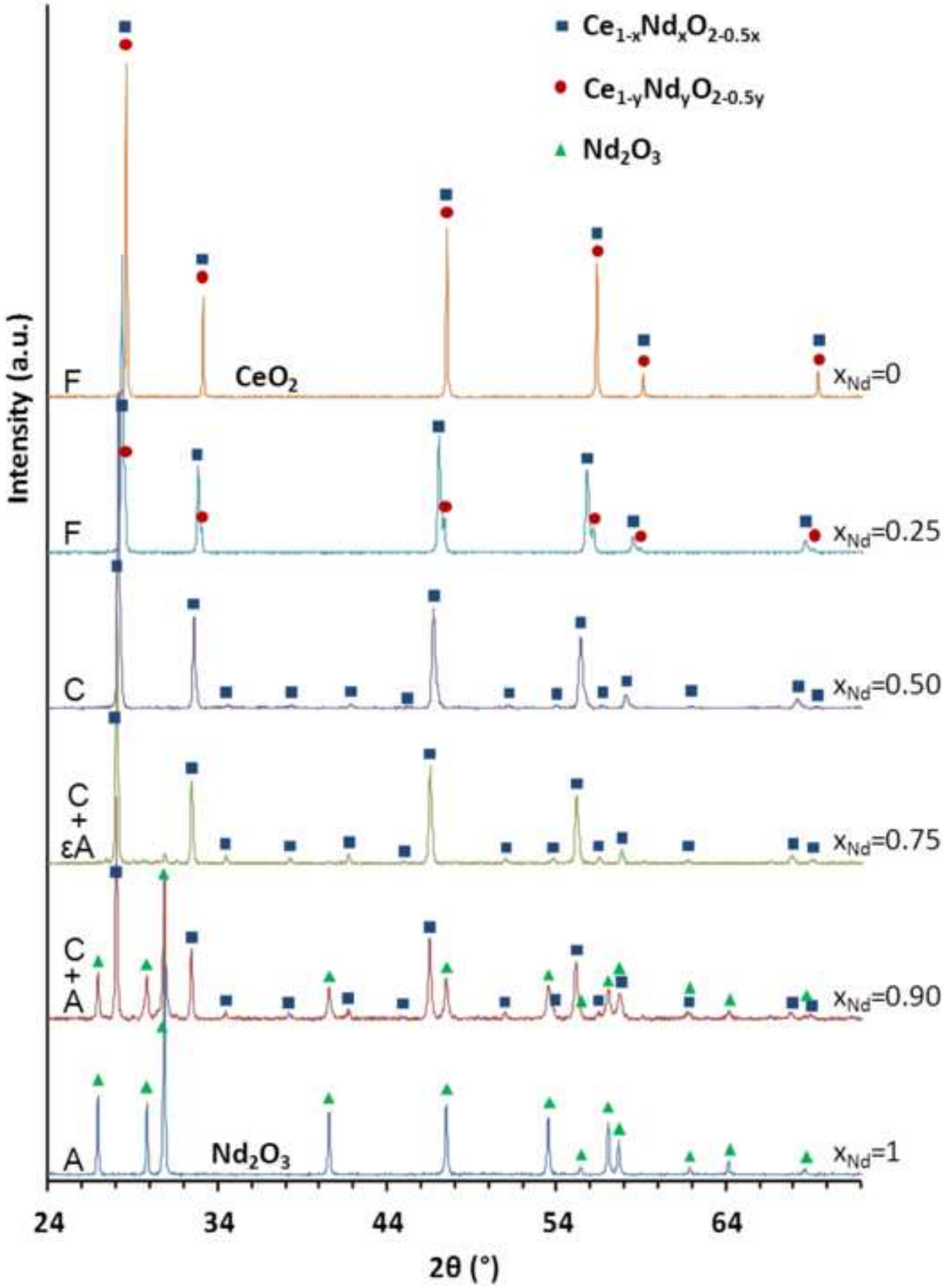

Figure 8

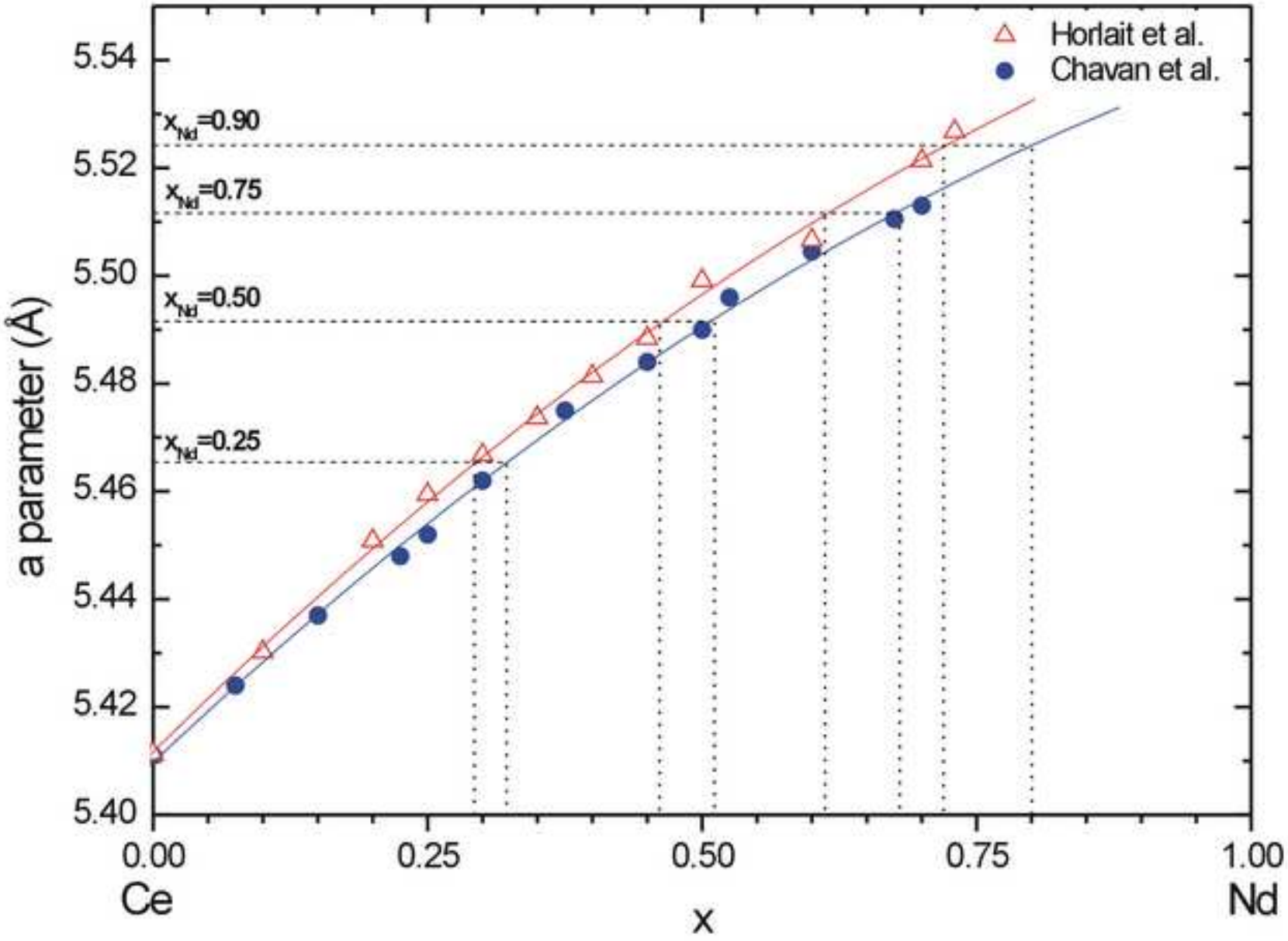

Figure 9

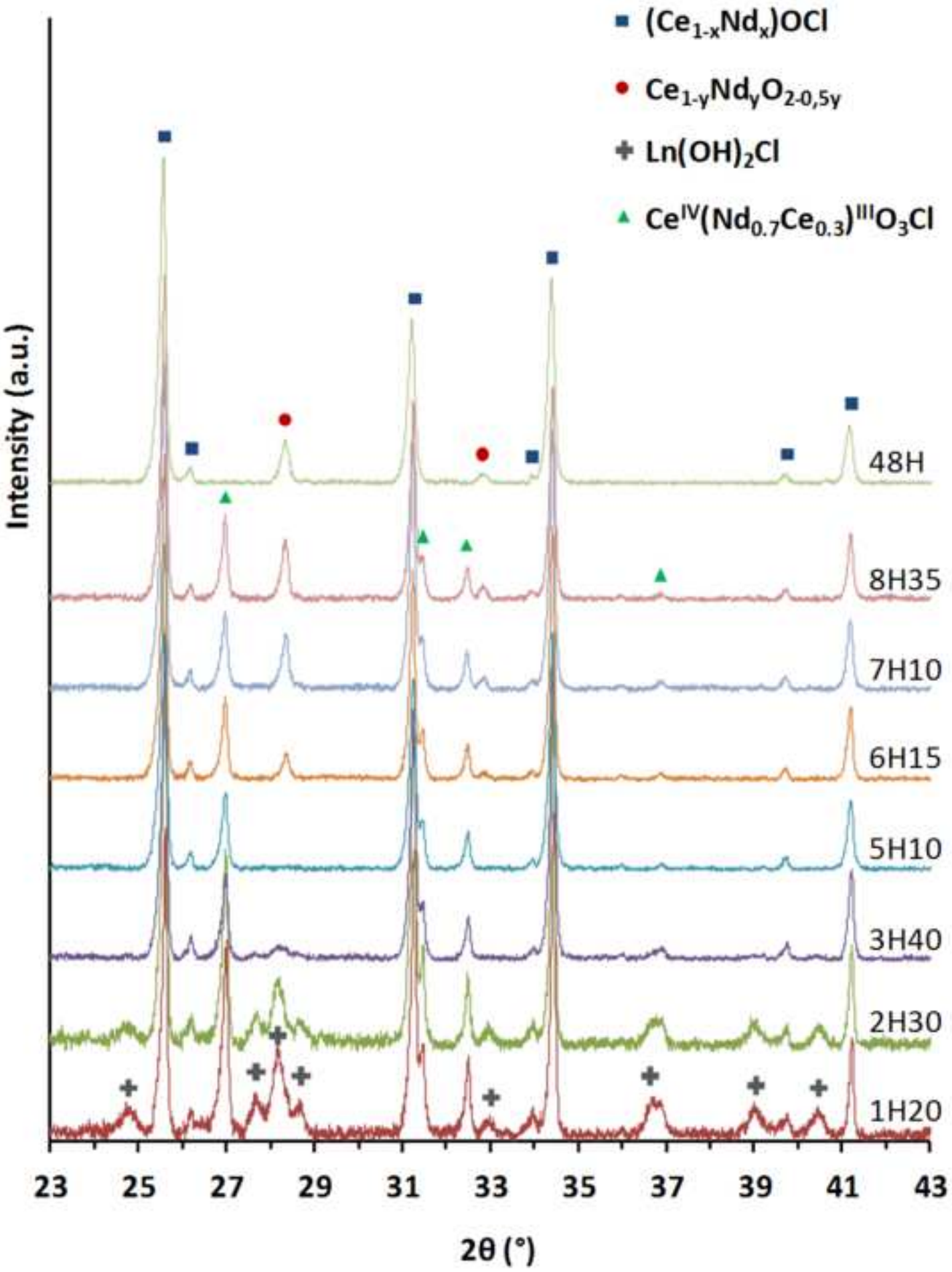

Table 1

experimental data		calculated data	
Ar flow rate	2 $L.h^{-1}$	H_2O partial vapor pressure	3169 Pa
H_2O temperature	25 °C	H_2O molar flow rate	0.0256 $mol.h^{-1}$
Soda solution volume	500 mL	Maximal HCl molar flow rate	0.0512 $mol.h^{-1}$
		Highest conductivity evolution	-1.25 $mS.cm^{-1}.h^{-1}$

Table 1: Experimental and calculated data for precipitation and the maximal conductivity evolution of the soda solution downstream the reactor.

Table 2

X_{Nd}	Ce precipitation yield (%)	Nd precipitation yield (%)
0.00	99.90(5)	-
0.25	99.80(5)	99.90(5)
0.50	99.90(5)	99.90(5)
0.75	99.90(5)	100.00(5)
1.00	-	99.90(5)

Table2 : Cerium and neodymium precipitation yields after 8 h wet argon sparging, determined by ICP analysis of unreacted cerium and neodymium.

Table 3

X_{Nd}	refined Cell parameter of oxides $Ce_{1-y}Nd_yO_{2-0.5y}$	y value of $Ce_{1-y}Nd_yO_{2-0.5y}$ deduced from [22,23]
0.00	5.4106(4)	0
0.25	5.4364(2)	0.15-0.12
0.50	5.4457(6)	0.20-0.17
0.60	5.4595(6)	0.29-0.25

Table 3 : Refinement cell parameters of oxides $Ce_{1-y}Nd_yO_{2-0.5y}$ from precipitation and deduced y values.

Table 4

Initial x_{Nd}	structure	Lattice parameter (Å)
0 .00	F-type $Fm\bar{3}m$	a=5.4118(1)
0.25	F-type $Fm\bar{3}m$	a=5.4654(1)
0.50	C-type $Ia\bar{3}$	a/2=5.4915(3)
0.75	C-type $Ia\bar{3}$	a/2=5.5116(4)
0.90	C-type $Ia\bar{3}$	a/2=5.5242(4)

Table 4 : Refined unit cell parameter of $Ce_{1-x}Nd_xO_{2-0.5x}$ depending on the initial lanthanides composition of the salt.

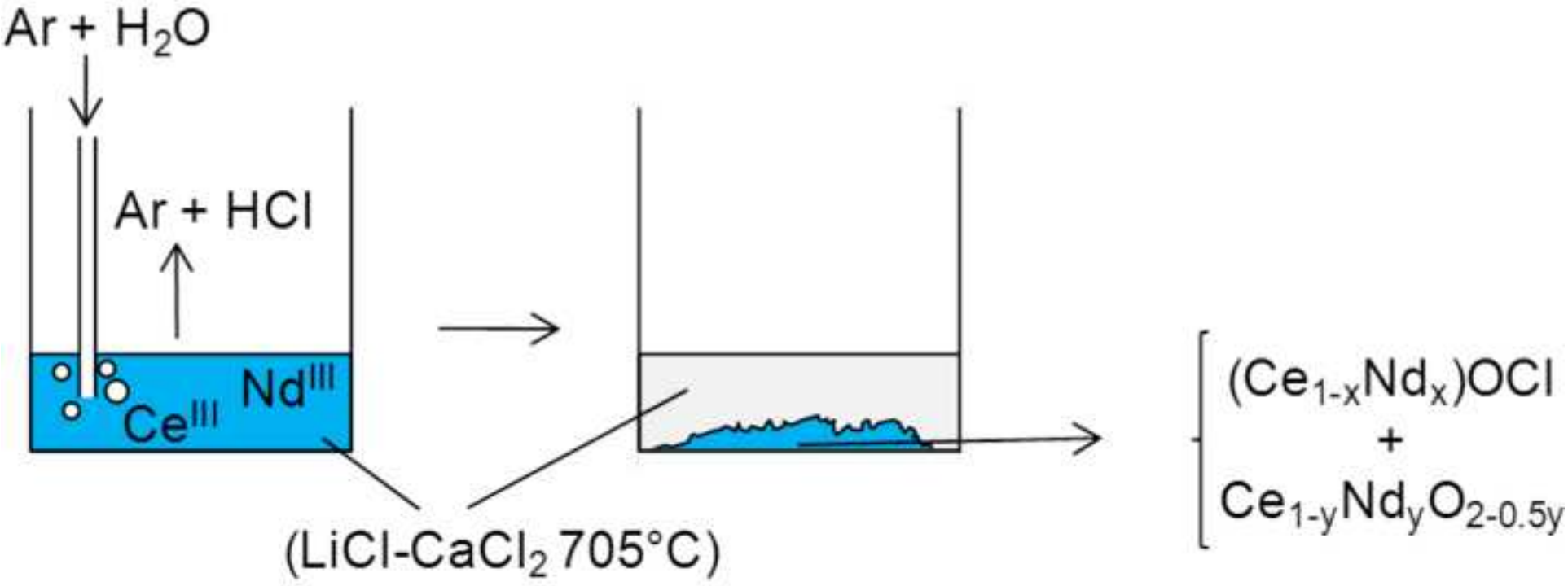
Ar + H_2O
Ar + HCl
Ce^{III}
Nd^{III}
($LiCl-CaCl_2$ 705°C)
$(Ce_{1-x}Nd_x)OCl$
+
$Ce_{1-y}Nd_yO_{2-0.5y}$